

# Mechanical Performance of Parallel Bamboo Strand Lumber Columns under Axial Compression: Experimental and Numerical Investigation

Cheng Tan<sup>a,b</sup>, Haitao Li<sup>a\*</sup>, Dongdong Wei<sup>c</sup>, Rodolfo Lorenzo<sup>d</sup>, Conggan Yuan<sup>c</sup>

<sup>a</sup> Collage of Civil Engineering, Nanjing Forestry University, Nanjing, China.

<sup>b</sup> Department of Civil and Environmental Engineering, Syracuse University, Syracuse, USA.

<sup>c</sup> Jiangxi Feiyu Bamboo Stock Co. LTD, Fengxin 330700, China.

<sup>d</sup> University College London, London WC1E 6BT, UK

\*Corresponding Author: Haitao Li. Email: lhaitao1982@126.com.

**Abstract:** This paper presents an investigation on the mechanical performance of parallel bamboo strand lumber (PBSL) columns under axial compression. Experimental test and numerical analysis were performed for 40 PBSL columns with various slenderness ratios. Failure modes, ultimate capacity and load-strain response are reported and evaluated. Strength failure is the typical failure mode of columns with small slenderness ratios, however, buckling failure is commonly observed for longer columns. Elastic eigenvalue analysis is found effective to predict critical buckling load of long columns, as buckling occurs within elastic range. However inelastic behavior has significant effect on critical load when the buckling stress exceeds proportional limit of the material. As a result, inelastic approaches provide more accurate prediction of critical load for columns with a slenderness ratio lower than the elastic threshold ( $\lambda_y$ ). The presented experimental results and numerical analysis validated the feasibility of the elastic/inelastic buckling analysis approaches on determination of ultimate capacity of axial loaded PBSL columns.

**Keywords:** Parallel bamboo strand lumber, axial compression, buckling, inelastic analysis.

## 1 Introduction

As an environmental friendly material, bamboo has been widely used as construction materials due to its excellent mechanical behavior [1], renewability and fast growing characteristic [2,3]. Compared to conventional construction materials, such as concrete, steel, and aluminium alloy, the strength-to-weight of bamboo is relatively high [4], which allows bamboo to be an efficient alternative of construction material.

The application of unprocessed bamboo is limited by its natural characteristics such as limited dimension, irregular shape and poor rigidity [5,6]. These drawbacks can be alleviated by reassembling the bamboo culms into desired forms with hot-pressure and adhesives [1,7], which referred as engineered bamboo. The most widely used two types of engineered bamboo are parallel bamboo strand lumber (PBSL) and laminated bamboo. Extensive studies have been conducted for engineered bamboo materials in terms of mechanical properties and engineering applications [8-26].

Mechanical properties of PBSL is significantly affected by the manufacturing process, raw material selection, moisture content and resin properties [1,8-10]. In general, mechanical properties of PBSL are comparable to or surpass that of traditional wood products [6]. In addition to material property investigation [11], extensive studies have been conducted on PBSL structural members in order to develop fundamental design, analysis and construction guidelines. Cui et al. [12-13] experimentally investigated the flexural behavior of PBSL beams and Huang et al. [14] developed a numerical analytical model to predict the bending performance of PBSL beams. Li et al. [5,15] investigated the mechanical performance of PBSL columns under eccentric loading, and proposed an eccentricity influencing coefficient to account for the eccentric effect. Huang et al. [16] proposed an iterative analytical model to predict ultimate

52 capacity of eccentrically loaded intermediate slenderness PBSL columns. Wang et al. [17]  
53 investigated the mechanical behavior of PBSL column under biaxial eccentric compression and  
54 developed an analytical model to predict the load-carrying capacity. Chen and Zhao [18-19]  
55 investigated the effect of holes with different shape, size and location on PBSL beams. Zhou et  
56 al.[20] performed an experimental study on the embedding strength of PBSL materials, test  
57 results shows the embedding strength is dominated by the bolt diameter. Cross-section size  
58 effect on compressive strength of PBSL columns was studied by Zhao [21] and a section-effect  
59 reduction factor was proposed.

60 There are a few studies on compressive behavior of PBSL columns, however, few study was  
61 conducted on buckling behavior of PBSL column with various slenderness ratios. In addition,  
62 current proposed critical load ( $P_{cr}$ ) analysis approaches of PBSL columns are based on linear  
63 elastic theory, non-linear effect on buckling behavior is rarely addressed or requires relative  
64 large amount of computational efforts.

65 This paper presents an experimental investigation of compressive behavior of PBSL columns  
66 with slenderness ratios ranging from 13.8 to 62.3 along with linear elastic and inelastic buckling  
67 analysis. Verification of the elastic/inelastic approach was made against experimental results.

## 68 **2 Experimental Tests**

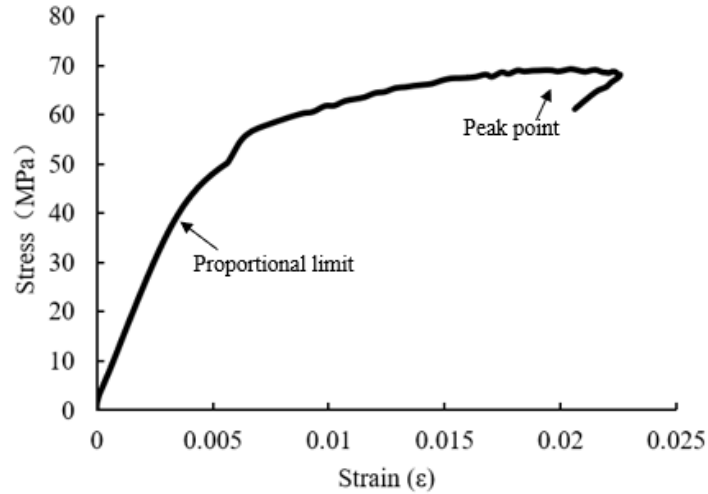
69 The experimental test consists of eight groups of specimens with different length (400 mm, 600  
70 mm, 800 mm, 1000 mm, 1200 mm, 1400 mm, 1600 mm and 1800 mm), as shown in Fig. 1. Each  
71 group consists of five identical specimens.



72  
73 Fig. 1. PBSL columns with various length

### 74 **2.1 Materials**

75 The raw bamboo material was Moso bamboo from Jiangxi Province, China. Bamboo strips  
76 were split into filament bundles and then charred at a temperature of 165 °C and a pressure of  
77 0.3 MPa. The dried and charred bamboo filament bundles were formed into a rectangular shape  
78 with Phenolic adhesives under 90 MPa transverse pressure and cured at a temperature of 140 °C.  
79 The density of the PBSL was reported as 1018 kg/m<sup>3</sup> and the water content was 8±1% on the  
80 day of testing. Specimens were cut and polished at laboratory of Nanjing Forestry University.  
81 According to the compressive test, the peak strength ( $f_u$ ) of is 63.92 MPa and the yield strength  
82 ( $f_y$ ) is 37.64 MPa. Compressive elastic modulus and Poisson's ratio are 11684.36 MPa and 0.39,  
83 respectively. Fig. 2. shows stress-strain relationship of the PBSL used in this study.



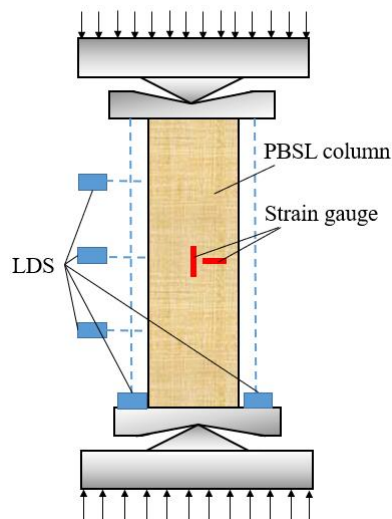
84  
85

Fig. 2. Stress-strain relationship

86 **2.2 Test setup and instrumentation**

87 Pin support was selected for both ends, as shown in Fig. 3. The applied load was recorded by  
88 the built-in load cell of the 1000kN electro-hydraulic testing machine. Longitudinal  
89 displacement was measured with laser displacement sensors (LDS) on opposite sides of the  
90 columns, the average of the two longitudinal LDS data was adapted for analysis. In addition,  
91 lateral displacement of the columns on quarter points were measured with LDS, dash lines in  
92 Fig. 3 show the direction of lasers. Longitudinal and transverse strain at mid-height were  
93 measured with strain gauges on all the four surfaces. All data were collected by the TDS-530  
94 data acquisition system. Fig. 4 shows the test setup of the column specimens.

95 Five cycles of pre-loading were performed for each specimen and specimen placement was  
96 adjusted until strain gauge on each surface showed similar values, which indicated the specimen  
97 was under pure axial loading. Load control was adapted before the columns reaching its linear  
98 proportional limit and it was switched to displacement control beyond the linear proportional  
99 limit at a rate of 3.6 mm/min.



100  
101

Fig. 3. Instrumentation



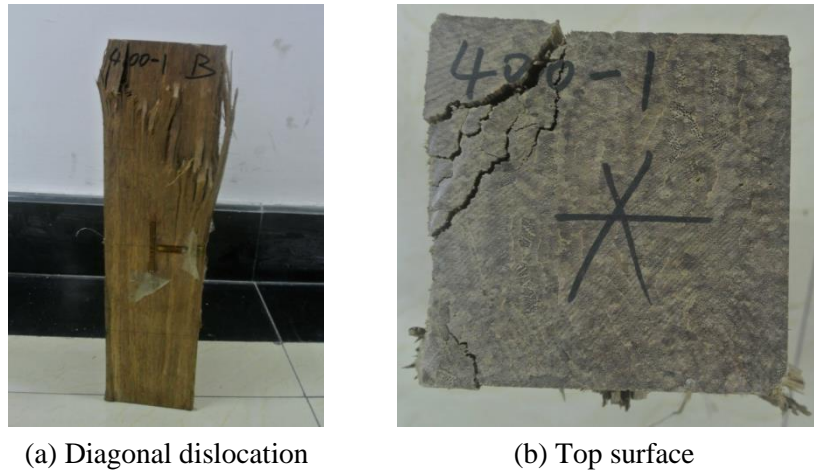
Fig. 4. Test setup

102 **3 Test Results and Discussion.**

103 **3.1 Failure mode and mechanism**

104 3.1.1 Strength failure

105 Strength failure, such as squashing or crushing of bamboo fibers, was the ultimate failure mode  
106 of columns with a slenderness ratio ( $\lambda$ ) smaller than 17, which referred as short columns [27].  
107 Tested columns remained linear elastic until 400 kN, yielding took place before  
108 crushing/squashing of the column (Fig. 9). At the failure stage, diagonal dislocation occurred  
109 near the end of columns, with fibers outwards splitting at corners, as shown in Fig. 5. Similar  
110 failure mode was observed for 600 mm height columns ( $\lambda = 20.72$ ).



113 Fig. 5. Strength failure

114 3.1.2 Buckling failure

115 For columns with a height larger than 600 mm, buckling dominated the ultimate failure, as  
116 shown in Fig. 6a. Large lateral deflection was observed at failure along with snapping of  
117 bamboo fibers at mid-height. For columns with a length ranging from 600-1400, apparent  
118 yielding before failure was observed (Fig. 9). However, for group 1600 mm and 1800 mm,  
119 yielding was not observed before buckling (Fig. 9). A few specimen failed in buckling along  
120 with severe splitting of the column from one end, as shown in Fig. 6b. This is attributed to large  
121 lateral deflection formed at mid-height, while lateral displacement was restrained at supports,  
122 internal stress was exerted to maintain compatibility.



123 (a) Large lateral deflection

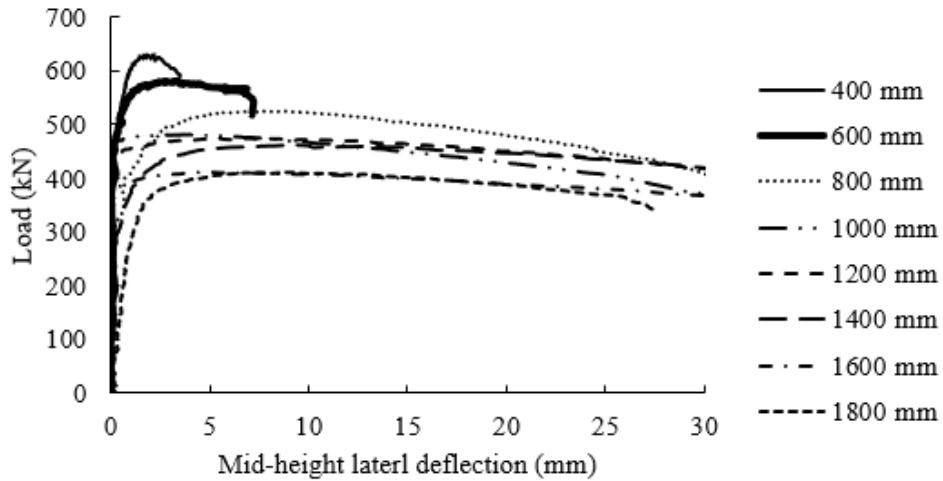
124 (b) Column splitting

125

Fig. 6. Buckling failure

126 **3.2 Ultimate capacity and lateral deflection**

127 Fig. 7 shows load versus lateral deflection at mid-height for specimens with various length. For  
128 short columns, no significant deflection was observed until reaching its ultimate capacity.  
129 However, for long columns, apparent deflection was observed before buckling occurred. Load  
130 capacity dropped gradually beyond the peak load until buckling.



131

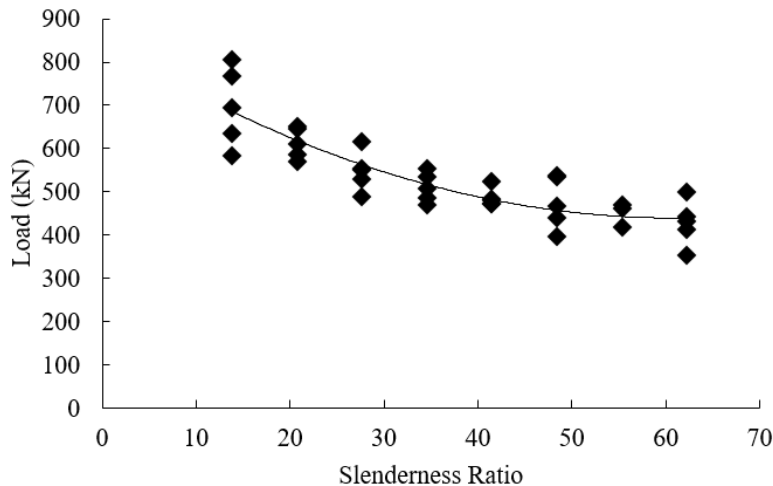
Fig. 7. Load vs lateral deflection

132

133 Ultimate capacity each group are summarized in Table. 1 and plotted in Fig. 8. Ultimate  
134 capacity was reduced significantly as slenderness ratio increased. Based on regression study,  
135 the ultimate capacity can be expressed by as Eq. 1.

136

$$P = 0.11\lambda^2 - 213.47\lambda + 850.92 \quad (1)$$



137

Fig. 8. Load capacity vs slenderness ratio

138

139 Where  $\lambda$  is slenderness ratio,

140

$$\lambda = L/\sqrt{I/A} \quad (2)$$

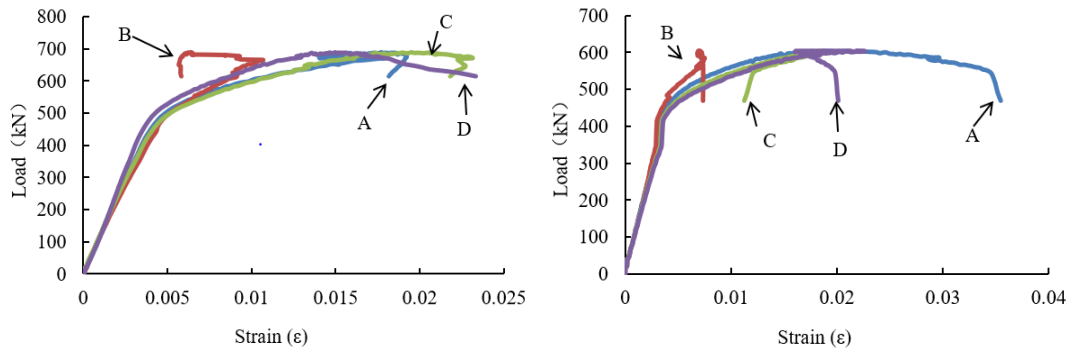
141

Where L is length of the column (mm); I and A are moment of inertia and area (mm<sup>4</sup>) of column cross-section (mm<sup>2</sup>).

142

143 **3.3 Strain analysis**

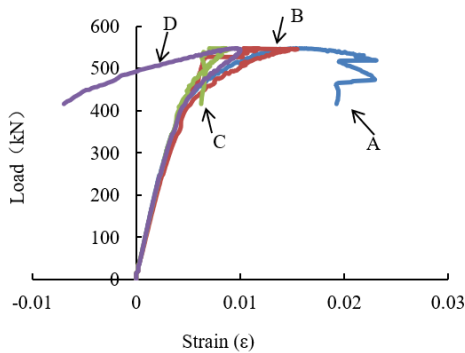
144 Fig. 9. shows load-longitudinal strain curves of each group of specimens. A, B, C and D  
 145 represents the four surfaces of the tested columns. It can be seen that for group 400 mm and  
 146 600 mm columns, which failed by strength failure, all surfaces are under compression.  
 147 For the rest groups, which failed in buckling, tensile strain was observed on the convex before ultimate  
 148 failure.



149  
 150

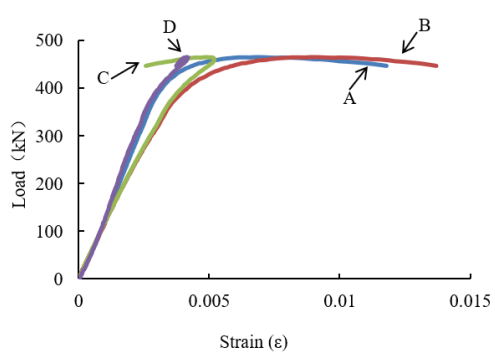
(a) 400-2

(b) 600-5

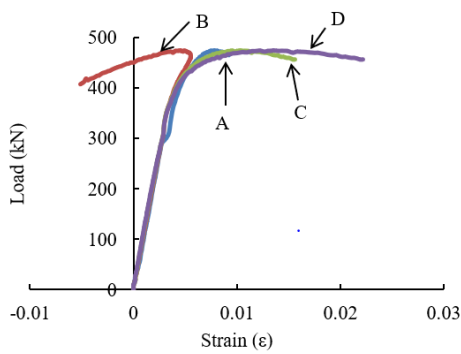


151  
 152

(c) 800-3

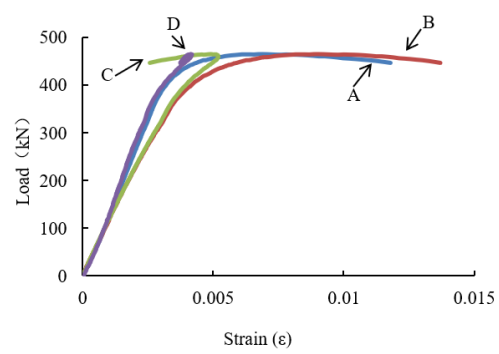


(d) 1000-2



153  
 154

(e) 1200-6



(f) 1400-2

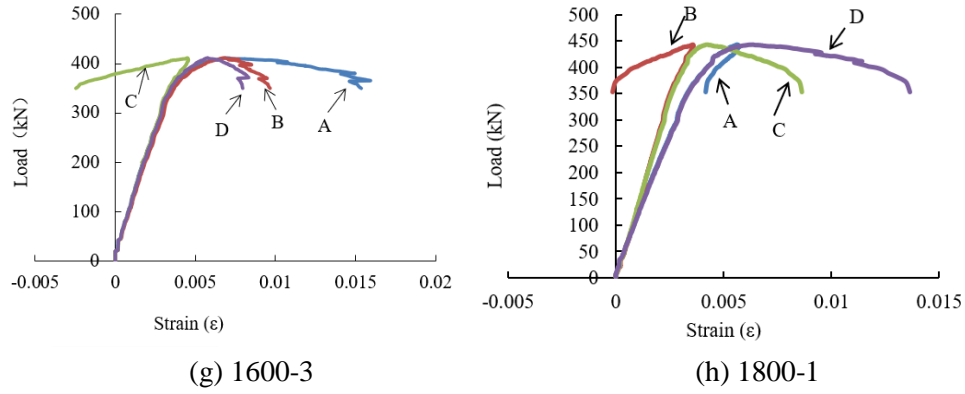


Fig. 9. Load-strain response

Maximum longitudinal/transverse strain of each group are summarized in Table. 1. Maximum longitudinal and transverse strain of PBSL column were reduced as slenderness ratio increased. For short columns failure by strength failure, compressive strength of PBSL were fully developed as the measured longitudinal strain was close to the ultimate compressive strain. However, for columns failure in buckling, compressive property was not fully developed. Fig. 10 and 11 show the maximum strain versus slenderness ratio. The usable strain was significantly reduced as the length of column increased. Relationship between longitudinal/transverse strain and slenderness ratio can be summarized by statistical regression analysis, as shown in Eq. 3 & 4.

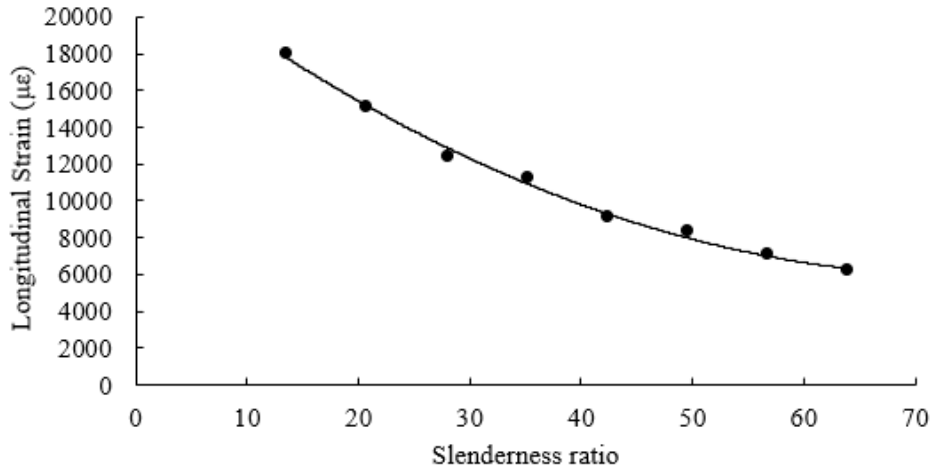
$$\varepsilon_l = 3.105\lambda^2 - 467.6\lambda + 23533 \quad (3)$$

$$\varepsilon_t = 1.476\lambda^2 - 283.2\lambda + 14350 \quad (4)$$

Where  $\varepsilon_l$  is the maximum longitudinal strain at mid height;  $\varepsilon_t$  is the maximum transverse strain at mid height;  $\lambda$  is slenderness ratio. Longitudinal strain should not exceed ultimate compressive strain of PBSL material and transverse strain should not exceed product of ultimate compressive strain and Poisson's ratio.

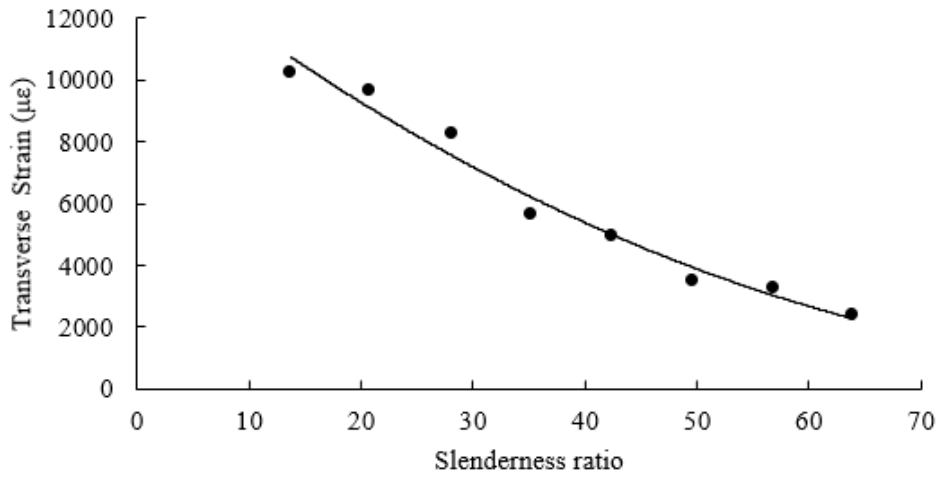
**Table 1:** Test results

Length (mm)	Slenderness ratio	Ultimate capacity (kN)	Average $\varepsilon_{l\ max}$	Average $\varepsilon_{t\ max}$
400	13.8	685.06	0.0181	0.0102
600	20.72	605.92	0.0153	0.0096
800	27.64	538.34	0.0122	0.0082
1000	34.58	502.26	0.0117	0.0056
1200	41.50	478.48	0.0094	0.0049
1400	48.45	467.02	0.0083	0.0035
1600	55.35	440.73	0.0072	0.0032
1800	62.26	423.20	0.0063	0.0024



176  
177

Fig. 10. Maximum longitudinal strain vs slenderness ratio



178  
179

Fig. 11. Maximum transverse strain vs slenderness ratio

180 **4 Analytical Models**

181 **4.1 Euler's equation**

182 By using the method of neutral equilibrium, the critical buckling load can be solved from the  
 183 governing differential equation for slight bent column configuration. In which, the column is  
 184 assumed to be perfectly straight and material obeys Hooke's Law (elastic). Small lateral  
 185 deflection allows the curvature can be expressed as second derivative of the lateral deflection.  
 186 The critical buckling load is solved through eigenvalue analysis as:

187 
$$P = \frac{n^2 \pi^2 EI}{L^2} \tag{5}$$

188 Where  $I$  is the moment of inertia of the cross-section and  $L$  is length of the column.

189 The value of  $P$  that corresponds to the smallest number  $n$  ( $n = 1$ ) is the critical buckling load  
 190 ( $P_{cr}$ ). Prediction of critical load with classic elastic Euler's equation and experiment results are  
 191 plotted in Fig. 12. It shows the critical load is significantly overestimated for short and



192 intermediate slender columns. However, as slenderness ratio approaching the elastic threshold  
193 ( $\lambda_y$ ), reasonable agreement could be achieved.

$$194 \quad \lambda_y = \pi\sqrt{E/f_y} \quad (6)$$

195 Where  $E$  is the compressive elastic modulus,  $f_y$  is the stress at proportional limit.

## 196 **4.2 Inelastic analysis**

### 197 *4.2.1 Tangent modulus and double modulus theory*

198 One of the assumptions used in Euler's equation is the material obeys Hooke's Law. However,  
199 this assumption is only valid for columns that are slender enough, so that buckling occurs before  
200 the proportional limit. For inelastically buckled columns, some fibers on the cross section yield  
201 before buckling occurs. As a result, additional load beyond proportional limit is resisted by a  
202 portion of the cross-section. The elastic modulus should be replaced by effective modulus, two  
203 widely used are tangent modulus and double modulus theory proposed by Engesser [28].

204 Other than assumptions addressed in elastic theory, it is assumed no strain reversal occurs  
205 during bending in tangent modulus theory. Tangent modulus ( $E_t$ ) of PBSL is determined as  
206 3531.48 MPa according to the stress-strain relation from the compressive property test. The  
207 critical load based on tangent modulus theory ( $P_t$ ) can be determined by Eq. 7.

$$208 \quad P_t = \frac{\pi^2 E_t I}{L^2} \quad (7)$$

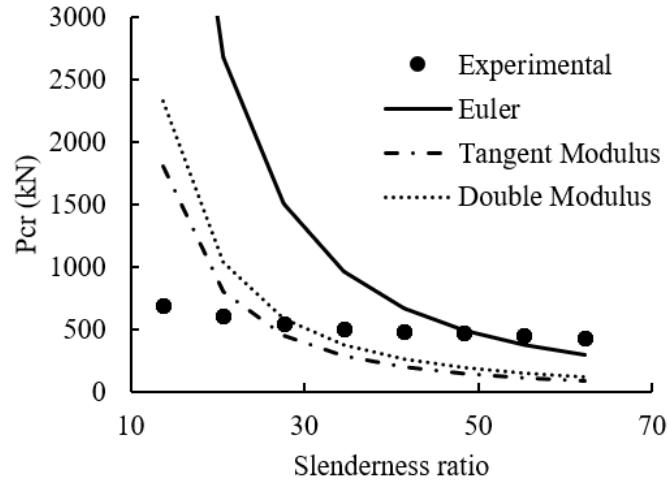
209 Double modulus theory, also referred as reduced modulus theory, was developed to address the  
210 strain reverse on the convex of the bended column. Fibers on convex tend to return to elastic  
211 stage, the section modulus is in between of elastic and tangent modulus. For rectangular  
212 sections, reduced modulus is

$$213 \quad E_r = \frac{4EE_t}{(\sqrt{E} + \sqrt{E_t})^2} \quad (8)$$

214 The critical load based on double modulus theory ( $P_r$ ) can be determined by Eq. 9.

$$215 \quad P_r = \frac{\pi^2 E_r I}{L^2} \quad (9)$$

216 Critical buckling load predicted using tangent/double modulus theory is plotted in Fig. 12. Both  
217 of the two approaches overestimate the capacity for short columns ( $\lambda < 20$ ) and underestimate  
218 the capacity for relative long columns ( $\lambda > 40$ ).



219  
220

Fig. 12. Comparison of theoretical and experimental results

#### 221 4.2.2 Newlin-Gahagan approach

222 Newlin-Gahagan approach [29] was developed for prediction of timber column buckling load.  
223 This approach has been proved to be efficient to predict inelastic buckling capacity of timber  
224 scrimber composite columns [30]. The critical stress ( $f_{cr}$ ) is expressed as a function of  
225 compressive stress ( $f_u$ ), proportional limit stress ( $f_y$ ), elastic threshold slenderness ratio ( $\lambda_y$ ) and  
226 actual slenderness ratio ( $\lambda$ ), all these properties could be achieved from the compressive stress-  
227 strain curve.

$$228 \quad f_{cr} = f_u \left[ 1 - \left( 1 - \frac{f_y}{f_u} \right) \left( \frac{\lambda}{\lambda_y} \right)^{\frac{2f_y}{f_u - f_y}} \right] \quad (10)$$

229 Critical buckling load can be calculated as the critical stress multiplied by the cross-section area.  
230 Prediction using Newlin-Gahagan approach is verified against experimental results, as shown  
231 in Fig. 13. It can be seen that the non-linear behavior can be accurately predicted by Newlin-  
232 Gahagan approach, however, for columns with large slenderness ratio, this method tends to  
233 underestimate the buckling load. The elastic threshold slenderness ratio can be used as a  
234 criterion to determine the applicability of this approach. For columns with slenderness ratio  
235 smaller than  $\lambda_y$ , whose ultimate capacity is dominated by inelastic behavior, the Newlin-  
236 Gahagan approach is applicable. Otherwise, the Euler's method is more suitable due to its  
237 reasonable accuracy and ease to apply.

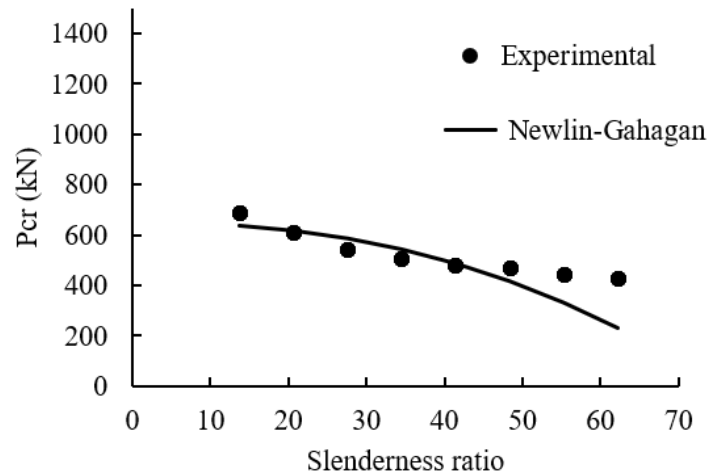


Fig. 13. Newlin-Gahagan approach

238  
239

## 240 5 Summary and Conclusion

241 Axial compressive tests were conducted for PBSL column with various slenderness ratios.  
242 Failure mode, ultimate capacity and load-strain response were reported. For columns with  
243 slenderness ratio lower than 20, strength failure was the typical failure model. No obvious later  
244 deflection was observed for the strength failed columns. For columns with slenderness ratio  
245 higher than 20, buckling dominates the failure mode. Ultimate capacity was reduced as the  
246 slenderness ratio increased. Significant lateral deflection was observed for buckling failed  
247 columns. According to the strain analysis, the compressive strength of PBSL could be almost  
248 fully developed for short columns ( $\lambda < 20$ ). However, for longer columns failed by buckling,  
249 lower strain value was observed which indicated that the compressive strength was not fully  
250 developed.

251 Applicability of Classic Euler's method, tangent modulus theory, double modulus theory and  
252 Newlin-Gahagan approach were investigated regarding to ultimate capacity prediction of axial  
253 loaded PBSL columns. Analysis result shows inelasticity has significant effect on columns with  
254 a slenderness ratio lower than  $\lambda_y$ . Newlin-Gahagan approach provides good predictions of  
255 ultimate capacity of inelastically failed columns. For columns with a slenderness ratio higher  
256 than  $\lambda_y$ , the classic Euler provides more accurate prediction than inelastic approaches.

257 **Acknowledgement:** This work was supported by the National Natural Science Foundation of  
258 China (51308301), the Natural Science Foundation of Jiangsu Province (No. BK20130978),  
259 the China Postdoctoral Science Foundation under Grant No. 2011M500930 and No.  
260 2013T60544, the Foundation of the Doctoral Program of the Ministry of Education under Grant  
261 No. 20123204120012, and a Project Funded by the Priority Academic Program Development  
262 of Jiangsu Higher Education Institutions. The authors declare having no significant competing  
263 financial, professional, or personal interests that might have influenced the performance or  
264 presentation of the work described in this paper. The authors gratefully acknowledge the help  
265 from faculties, staff and students of Nanjing Forestry University.

## 266 References

- 267 [1] M. Ahmad, F. Kamke. Properties of parallel strand lumber from Calcutta bamboo  
268 (Dendrocalamus strictus). Wood Sci. Technol. 45(1) (2011) 63-72.  
269 [2] P. Van der Lugt, Van den Dobbeksteen, J. Janssen. An environmental, economic and  
270 practical assessment of bamboo as a building material for supporting structures. Constr.

- 271 Build. Mater. 20(9) (2006) 648-656.
- 272 [3] A. Porras, A. Maranon. Development and characterization of a laminate composite material  
273 from polylactic acid (PLA) and woven bamboo fabric. *Composites Part B* 43(7) (2012)  
274 2782-2788.
- 275 [4] M. Mahdavi, P. Clouston, S. Arwade.(2010): Delvelopment of laminated bamboo lumber:  
276 review of processing, performance and economical considerations. *J. Mater. Civ. Eng.* 23(7)  
277 (2010) 1036-1042.
- 278 [5] H. Li, J. Su, A. Deeks, Q. Zhang, D. Wei, C. Yuan. Eccentric compression performance of  
279 parallel bamboo strand lumber columns. *BioResour.* 10(4) (2015) 7065-7080.
- 280 [6] B. Sharma, A. Gatóo, M. Bock, M. Ramage. Engineered bamboo for structural applications.  
281 *Constr. Build. Mater.* 81 (2015) 66-73.
- 282 [7] X. Li, M. Ashraf, H. Li, X. Zheng, A. Ameri. Behavior of parallel bamboo strand lumber  
283 under compression loading - an experimental study. *MATEC Web of Conferences* (2019)  
284 275.
- 285 [8] P. Malanit, M. Barbu, A. Frühwald. Physical and mechanical properties of oriented strand  
286 lumber made from an Asian bamboo (*Dendrocalamus asper* Backer). *Eur. J. Wood and*  
287 *Wood Prod.* 69(1) (2010) 27-36.
- 288 [9] A. Kumar, T.Vlach, L. Laiblova, B. Hrouda, J. Tywoniak, P. Hajek. (2016): Engineered  
289 bamboo scrimber: Influence of density on the mechanical and water absorption properties.  
290 *Constr. Build. Mater.*127 (2016) 815-827.
- 291 [10] R. Kurt, E. Tomak. The effect of DMDHEU modification on physical and biological  
292 properties of parallel strand lumbers. *Constr. Build. Mater.* 195 (2019) 597-504.
- 293 [11] D.Huang, Y. Bian, A. Zhou, B.; Sheng. Experimental study on stress-strain relationships  
294 and failure mechanisms of parallel strand bamboo made from *phyllostachys*. *Constr. Build.*  
295 *Mater.*77 (2015) 130-138.
- 296 [12] H. Cui, M. Guan, Y. Zhu. The flexural characteristics of prestressed bamboo slivers  
297 reinforced parallel strand lumber (PSL). *Key Engi. Mater.* 517 (2012) 96-100.
- 298 [13] H.Zhang, H. Li, I. Corbi, O. Corbi, G. Wu, C. Zhao, T. Cao. AFRP influence on parallel  
299 bamboo strand lumber beams. *Sensors* 18(9) (2018) 2854.
- 300 [14] D. Huang, A. Zhou, Y. Bian, Y. Sheng. Experimental and analytical study on the nonlinear  
301 bending of parallel strand bamboo beams. *Constr. Buid. Mater.* 44 (2013) 585-592.
- 302 [15] H. Li, Z. Qiu, G. Wu, O. Corbi, L. Wang, I. Corbi, C. Yuan. Slenderness ratio effect on  
303 eccentric compression performance of parallel strand bamboo lumber columns. *J. Struct.*  
304 *Eng. ASCE.*, 145(8) (2019) 04019077
- 305 [16] D. Huang, Y. Bian, D. Huang, A. Zhou, B. Sheng. An ultimate-state-based-model for  
306 inelastic analysis of intermediate slenderness PSB columns under eccentrically  
307 compressive load. *Constr. Build. Mater.* 94 (2015) 306-314.
- 308 [17] X. Wang, A. Zhou, Y. Chui. Load-carrying capacity of intermediately slender parallel  
309 strand bamboo columns with a rectangular cross section under biaxial eccentric  
310 compression. *Bioresour.* 13(1) (2018) 313-330.
- 311 [18] G. Chen, H. Li, T. Zhou, C. Li, Y. Song, R. Xu. Experimental evaluation on mechanical  
312 performance of OSB webbedparallel strand bamboo I-joist with holes in the web. *Constr.*  
313 *Build. Mater.* 101 (2015) 91-98.
- 314 [19] J. Zhao, Z. Meng, Z. Jin, D. Chen, Y. Wu, W. Zhang. Bending properties of bamboo

315       scrimber with holes in different sizes and positions. *Constr. Build. Mater.* 200 (2019) 209-  
316       217.

317 [20] J. Zhou, D. Huang, Y. Song, C. Ni. Experimental investigation on embedding strength  
318 perpendicular to grain of parallel strand bamboo. *Adv. in Mater. Sci. Eng.* 8 (2018).

319 [21] P. Zhao, X. Zhang. Size effect of section on ultimate compressive strength parallel to grain  
320 of structural bamboo scrimber. *Constr. Build. Mater.* 200 (2019) 586-590.

321 [22] H. Li, Q. Zhang, D. Huang, A.J. Deeks. Compressive performance of laminated bamboo.  
322 *Composites Part B* 54(1) (2013) 319-328.

323 [23] H. Li, J. Su, Q. Zhang, A. Deeks, D. Hui. Mechanical performance of laminated bamboo  
324 column under axial compression. *Composite Part B* 79 (2015) 374-382.

325 [24] H. Li, G. Wu, Q. Zhang, J. Su. Mechanical evaluation for laminated bamboo lumber along  
326 two eccentric compression directions. *J. wood sci.* 62(6) (2016) 503-517.

327 [25] H. Li, G. Chen, Q. Zhang, M. Ashraf, B. Xu, Y. Li. Mechanical properties of laminated  
328 bamboo lumber column under radial eccentric compression. *Constr. Build. Mater.* 121  
329 (2016) 644-652.

330 [26] H. Li, G. Wu, Q. Zhang, A.J. Deeks, J. Su. Ultimate bending capacity evaluation of  
331 laminated bamboo lumber beams. *Constr. Build. Mater.* 160 (2018) 365-375.

332 [27] ASTM. D198-15 Standard test methods of static tests of lumber in structural sizes.  
333 American Society for Testing and Materials. 2015.

334 [28] W. Chen, E. Lui. *Structural Stability: Theory and Implementation*. Upper Saddle River,  
335 NJ: Prentice-Hall, Inc. (1987).

336 [29] J. Newlin, J. Gahagan. Tests of large timber columns and presentation of the forest  
337 products laboratory column formula. *U. S Dep Agric Tech Bull.* (1930).

338 [30] Z. Li, M. He, D. Tao, M. Li. Experimental buckling performance of scrimber composite  
339 columns under axial compression. *Composite Part B* 86 (2016) 203-213.